MYELOID NEOPLASIA

PKR inhibits the DNA damage response, and is associated with poor survival in AML and accelerated leukemia in NHD13 mice

Xiaodong Cheng,[1,2,*] Michael Byrne,[1-3,*] Kevin D. Brown,[2,4] Marina Y. Konopleva,[5] Steven M. Kornblau,[5] Richard L. Bennett,[1,2,†] and W. Stratford May[1,2,†]

[1]Department of Medicine, Division of Hematology and Oncology, Department of Medicine, University of Florida, Gainesville, FL; and [2]University of Florida Health Cancer Center, Gainesville, FL; [3]Division of Hematology-Oncology, Vanderbilt University Medical Center, Nashville, TN; [4]Department of Biochemistry and Molecular Biology, University of Florida, Gainesville, FL; and [5]Department of Leukemia, The University of Texas MD Anderson Cancer Center, Houston, TX

Key Points

- Nuclear PKR activity represses DNA damage response signaling and DNA repair in primary hematopoietic cells.
- Increased PKR promotes genomic instability and inferior outcomes in both AML and the NHD13 mouse model of leukemia.

Increased expression of the interferon-inducible double-stranded RNA-activated protein kinase (PKR) has been reported in acute leukemia and solid tumors, but the role of PKR has been unclear. Now, our results indicate that high PKR expression in CD34$^+$ cells of acute myeloid leukemia (AML) patients correlates with worse survival and shortened remission duration. Significantly, we find that PKR has a novel and previously unrecognized nuclear function to inhibit DNA damage response signaling and double-strand break repair. Nuclear PKR antagonizes ataxia-telangiectasia mutated (ATM) activation by a mechanism dependent on protein phosphatase 2A activity. Thus, inhibition of PKR expression or activity promotes ATM activation, γ-H2AX formation, and phosphorylation of NBS1 following ionizing irradiation. PKR transgenic but not PKR null mice demonstrate a mutator phenotype characterized by radiation-induced and age-associated genomic instability that was partially reversed by short-term pharmacologic PKR inhibition. Furthermore, the age-associated accumulation of somatic mutations that occurs in the Nup98-HOXD13 (NHD13) mouse model of leukemia progression was significantly elevated by co-expression of a PKR transgene, whereas knockout of PKR expression or pharmacologic inhibition of PKR activity reduced the frequency of spontaneous mutations in vivo. Thus, PKR cooperated with the NHD13 transgene to accelerate leukemia progression and shorten survival. Taken together, these results indicate that increased nuclear PKR has an oncogenic function that promotes the accumulation of potentially deleterious mutations. Thus, PKR inhibition may be a therapeutically useful strategy to prevent leukemia progression or relapse, and improve clinical outcomes. (*Blood*. 2015;126(13):1585-1594)

Introduction

The double-stranded RNA-activated protein kinase (PKR) can be activated by a variety of cellular stresses to play a pivotal role in proapoptotic and inflammatory signaling pathways.[1-11] Due to proapoptotic functions, PKR has been considered to have tumor suppressor properties. However, PKR knockout mice (PKRKO) do not display any increased tumor incidence.[12] In addition, we recently discovered that mice expressing a PKR transgene (transgenic PKR [TgPKR]) specifically in hematopoietic cells develop a preleukemic, myelodysplastic syndrome (MDS)-like phenotype that includes bone marrow (BM) dysplasia and increased BM blasts.[3] Furthermore, increased PKR has been reported in patients with acute leukemias, as well as breast, melanoma, and colon cancers.[13-17] Thus, PKR may have a previously unrecognized role that contributes to oncogenesis.

Although the role of PKR in the cytoplasm to inhibit protein synthesis has been well studied, at least 20% of PKR resides in the nucleus but the function of nuclear PKR is unclear.[18] Increased nuclear PKR activity is found in CD34$^+$ blasts from high-risk MDS patients but not from low-risk MDS patients or healthy donors, and PKR is mainly nuclear in phosphatase and tensin homologue-deficient acute leukemia cell lines, suggesting that nuclear PKR signaling may play a role in tumorigenesis.[17,19,20] Since we recently observed that Lineage-negative (Lin$^-$) cells isolated from BM of TgPKR mice are more sensitive, whereas cells from PKRKO mice are highly resistant to genotoxic stresses including ionizing irradiation (IR),[3] we investigated whether nuclear PKR may regulate DNA damage response (DDR) signaling and whether decreased PKR expression/activity may safeguard genomic fidelity.

Materials and methods

Acquisition and analysis of acute myeloid leukemia (AML) patient samples

Peripheral blood (PB) and BM were collected from 414 patients with newly diagnosed AML at The University of Texas M. D. Anderson Cancer Center

Submitted March 18, 2015; accepted June 25, 2015. Prepublished online as *Blood* First Edition paper, July 22, 2015; DOI 10.1182/blood-2015-03-635227.

*X.C. and M.B. are co-first authors.

†R.L.B. and W.S.M. are co-senior authors.

The online version of this article contains a data supplement.

There is an Inside *Blood* Commentary on this article in this issue.

The publication costs of this article were defrayed in part by page charge payment. Therefore, and solely to indicate this fact, this article is hereby marked "advertisement" in accordance with 18 USC section 1734.

between September 1999 and March 2007 during routine diagnostic assessments under Institutional Review Board-approved protocol 05-0654. Informed consent was obtained in accordance with the Declaration of Helsinki. Proteomic profiling of PKR in $CD34^+$ cells was performed by reverse phase protein array (RPPA) using the PKR M02 monoclonal antibody, clone 1D11 (Abnova, Taipei, Taiwan). Isolation of $CD34^+$ cells from patient samples, RPPA processing, and statistical analysis was performed as described.[21,22] In addition, $CD34^+$ cells were isolated from an independent set of 6 randomly selected AML patients by positive selection using a CD34 MicroBead Kit (Miltenyi Biotec, Auburn, CA), and primary human $CD34^+$ isolated from the BM of healthy donors were purchased from Lonza (Walkersville, MD). Measurement of PKR gene expression in $CD34^+$ AML and normal cells is described in supplemental Methods on the *Blood* Web site.

Mice

C57BL/6-Tg (*Vav-NUP98/HOXD13*) (NHD13) mice were purchased from The Jackson Laboratory (#010505; Bar Harbor, ME). PKR (TgPKR) and PKRKO mice were described previously.[3] Breeding to generate NHD13-TgPKR and NHD13-PKRKO, and genotyping and analysis of PB and BM for evidence of MDS/leukemia is described in supplemental Methods. In addition, treatment of mice with PKR inhibitor (PKRI) is described in supplemental Methods. The University of Florida Institutional Animal Care and Use Committee approved these experiments (#201102224 and #201208669).

Cell lines, antibodies, and other reagents

REH, K562, and HL60 cells were from American Type Culture Collection (Manassas, VA) and propagated under standard growth conditions.[11] Generation of cell lines expressing short hairpin RNA (shRNA) is described in supplemental Methods. PKRI compound, okadaic acid (OA), and anti-phospho(serine 1981)-ataxia-telangiectasia mutated (p-ATM) antibody, clone 10H11.E12, were purchased from EMD Millipore (Darmstadt, Germany). FTY720 was obtained from Cayman Chemical Company (Ann Arbor, MI). Antibodies for actin, HSP90 protein phosphatase 2A (PP2A)/C, PP2A-B55α, and PP2A-B56γ were purchased from Santa Cruz Biotechnology (Santa Cruz, CA). p-PKR (threonine 451) antibody was purchased from Invitrogen/BioSource (Grand Island, NY). Antibodies for H2AX, γ-H2AX, ATM, LSD1, NBS1, and p-NBS1 (serine 343) were purchased from Cell Signaling Technology (Beverly, MA).

Flow cytometry

Staining of surface antigens was performed as described.[3] For staining of intracellular antigens, cells were fixed with 1% methanol-free formaldehyde, washed with phosphate-buffered saline (PBS), and permeabilized with 70% ethanol. After washing with PBS containing 1% bovine serum albumin and 0.02% Tween 20, cells were stained with primary antibody overnight at 4°C, and washed and stained with fluorochrome-conjugated secondary antibody. Flow cytometry was performed on an Accuri C6 flow cytometer at the University of Florida core facility (BD Biosciences, San Jose, CA).

Immunofluorescence (IF) microscopy

Cell cytospins were prepared, fixed with 4% paraformaldehyde for 30 minutes, permeabilized with 1% Triton in PBS for 10 minutes and stained with a 1:30 dilution of the indicated primary antibody, and 1:100 dilution of fluorochrome-conjugated secondary antibody. Slides were mounted with ProLong Gold antifade reagent containing 4,6 diamidino-2-phenylindole (DAPI, Life Technologies, Grand Island, NY) and viewed with a Zeiss Axioplan 2 microscope equipped with epifluorescence optics at ×63. Images were captured using Openlab 5.

Nuclear fractionation, immunoblotting, and immunoprecipitation (IP)

Nuclear and cytoplasmic subcellular fractions were prepared using an NE-PER Kit according to the manufacturer's protocol (Pierce, Rockford, IL). Sodium dodecyl sulfate-polyacrylamide gel electrophoresis and immunoblotting was performed as previously described.[11] For IP, 500 μg of protein lysate was precleared with nonspecific mouse immunoglobulin (Ig)G and protein G, then incubated overnight with the indicated antibody (1:100 dilution) and protein G agarose (Life Technologies, Grand Island, NY) at 4°C. Agarose-conjugated complexes were washed with PBS and detected by immunoblotting as described.[11] PP2A was immunoprecipitated from nuclear extracts and activity assayed using a PP2A IP phosphatase kit (17-313; Millipore, Billerica, MA) according to the manufacturer's protocol and as previously described.[11]

Measurement of DNA repair following IR

DNA repair was quantified using a Comet Assay Kit and neutral conditions according to the manufacturer's protocol (Trevigen, Gaithersburg, MD). SYBR green-stained slides were observed at ×40 by fluorescence microscopy using the equipment and software described above. Comet Olive Tail Moment calculations were performed on 50 randomly chosen cells for each sample by Wimasis Image Analysis (Munich, Germany).

Statistical analysis

Data are presented as the mean ± standard error of the mean of at least 3 independent experiments. Significance ($P < .05$) was determined by Student *t* test using Prism 6 (GraphPad Software, La Jolla, CA). Kaplan–Meier analysis and Cox proportional hazard modeling were performed on RPPA results using Statistica Version 10 (StatSoft). Kaplan–Meier and Log-rank analysis of mice were performed using Prism 6.

Results

PKR expression correlates with inferior survival and shorter remission duration for AML patients

Increased PKR expression and activity have been reported in leukemia patient samples and leukemia-derived cell lines.[16,17,20] To elucidate the role of PKR in leukemia, we tested whether PKR expression may be associated with clinical outcome by RPPA analysis of primary $CD34^+$ blast cells from 414 newly diagnosed AML patients.[22,23] When stratified for PKR, AML patients with the highest one-third of PKR expression in $CD34^+$ cells had a significantly worse overall survival (OS) than patients with the lowest two-third of PKR expression (Figure 1A) (median survival 41.6 vs 54.6 weeks; $P < .05$). Furthermore, patients with low PKR expression were approximately twice as likely to remain in remission after 2 years compared with patients with high PKR expression (Figure 1B). These correlations were most significant for AML patients with unfavorable cytogenetics (Figure 1C-D and supplemental Figure 1), and are similar to other published reports and those in curated databases such as www.oncomine.org and www.kmplot.com, which indicate that high PKR expression is found in tumor vs normal tissues and correlates with reduced survival in large cohort studies of breast, lung, and ovarian cancer patients (supplemental Figure 2).[13-16] Because PKR's reported proapoptotic function cannot readily account for these findings, we examined whether PKR may have a previously unrecognized oncogenic function.

PKR inhibits DDR signaling

Because we previously demonstrated that cells from PKRKO mice or treated with a pharmacologic PKRI are resistant to genotoxic stress,[3,11] we tested whether PKR may regulate DDR signaling in primary $CD34^+$ cells isolated from BM of AML patients or healthy donors, murine Lin^- BM cells, and leukemia cell lines. As a measure of DDR signaling, ATM autophosphorylation on serine 1981 (*p*-ATM), phosphorylation of histone H2AX (γ-H2AX), and phosphorylation

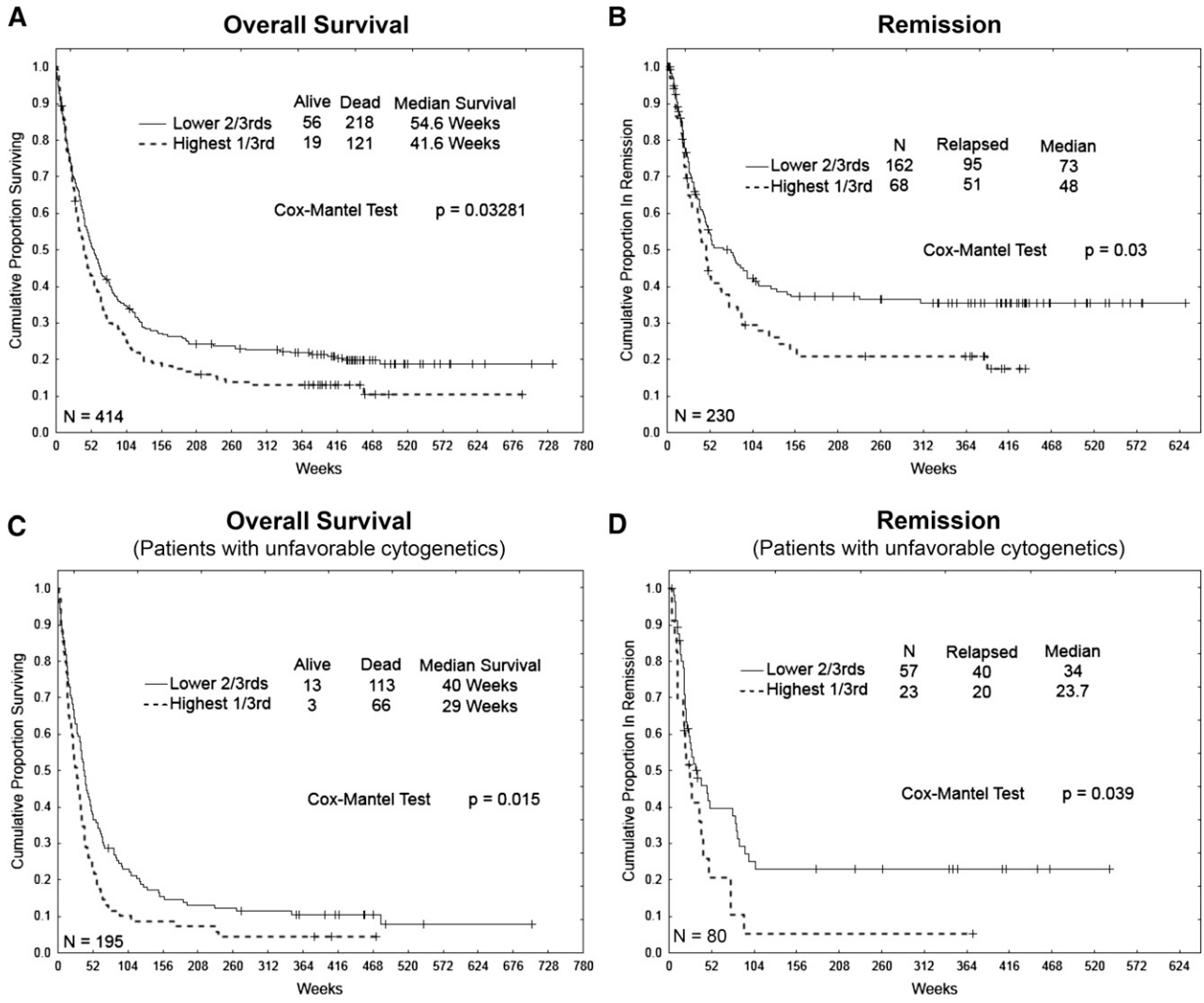

Figure 1. Increased PKR expression is associated with poor survival and shortened remission for acute leukemia patients. RPPA of $CD34^+$ cells collected from PB and BM of 414 newly diagnosed AML patients was used to classify patients into 2 groups based on PKR expression level (highest one-third vs lowest two-third expression). Kaplan-Meier analysis was used to measure: (A) OS probability of all patients (n = 414), (B) remission duration for those patients who achieved complete remission (n = 230), (C) survival probability for those patients with unfavorable cytogenetics (n = 195), and (D) remission duration of patients with unfavorable cytogenetics (n = 80). Median (weeks) and *P* value for each group were calculated by Cox proportional hazard modeling (ie, Cox-Mantel test).

of the ATM target NBS1 (*p*-NBS1) on serine 343 were examined by western blotting, IF microscopy, and flow cytometry (supplemental Figure 3A-C).[24-26]

Phospho(threonine 451)-PKR (p-PKR), indicative of activated PKR,[27] was observed in the nucleus of $CD34^+$ cells isolated from BM or PB of 6 AML patients, and treatment with a PKRI effectively decreased activated but not total PKR (supplemental Figure 3D and data not shown). Furthermore, IF staining and flow cytometry demonstrated that PKRI treatment increased *p*-ATM, γ-H2AX, and *p*-NBS1 in primary $CD34^+$ AML cells after IR (Figure 2A-C). In addition, the rate and abundance of γ-H2AX foci formation following IR, as well as resolution of foci, was increased by PKRI treatment of $CD34^+$ AML cells compared with control cells (Figure 2D). Significantly, when the percentage of cells positive for γ-H2AX or *p*-ATM after IR was plotted against relative PKR expression for each AML sample, patients with the highest PKR expression in $CD34^+$ BM cells displayed the lowest IR-induced γ-H2AX and *p*-ATM (Figure 2E-F). In support of this, the inhibition of PKR activity by either PKRI treatment or knockdown of PKR expression by shRNA in primary $CD34^+$ cells also demonstrated increased IR-induced γ-H2AX and *p*-ATM formation (Figure 2G-H and supplemental Figure 3F-K). Thus, an inverse relationship exists between PKR and DDR signaling in primary human $CD34^+$ hematopoietic stem and progenitor cells from AML patients or healthy donors.

To determine whether increased PKR expression inhibited DDR signaling in primary hematopoietic cells, we compared DDR signaling following IR in Lin^- cells collected from the BM of TgPKR, PKRKO, and wild-type (WT) mice. Lin^- cells isolated from the BM of TgPKR mice show a significantly impaired rate and amplitude of γ-H2AX formation compared with cells from WT or PKRKO mice (Figure 2I). Furthermore, Lin^- cells from TgPKR mice have a decreased percentage of cells positive for *p*-ATM and *p*-NBS1 (Figure 2J-K), and treatment of TgPKR Lin^- BM cells with PKRI restored DDR signaling to the level of WT Lin^- cells (supplemental Figure 3E and data not shown).

Next, we tested whether PKR expression or activity was required to regulate DDR signaling in leukemic cell lines. Knockdown of PKR in REH, K562, or HL60 cells (supplemental Figure 3L) promoted more rapid γ-H2AX formation and significantly increased *p*-ATM and *p*-NBS1 following IR as compared with control cells

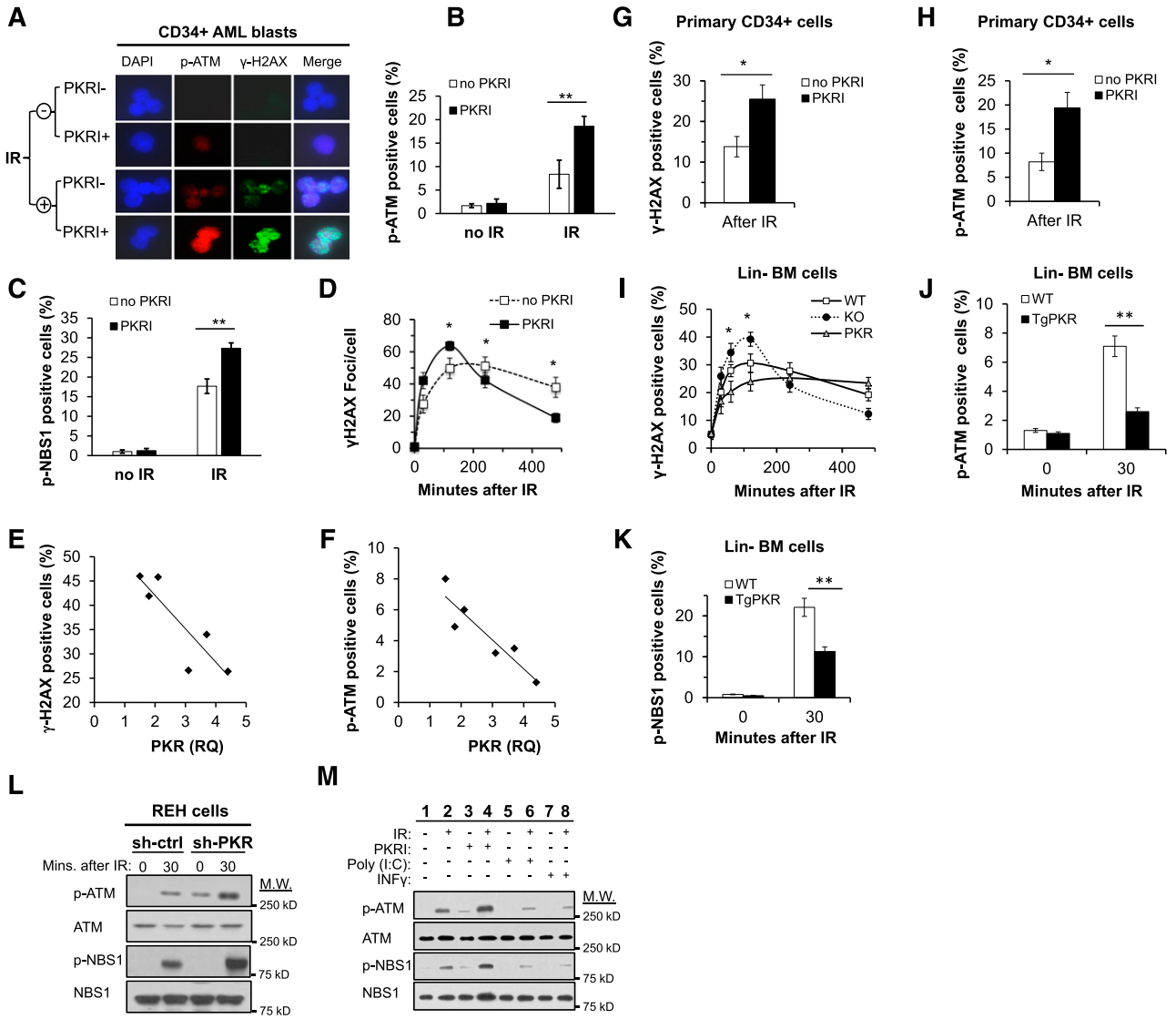

Figure 2. PKR inhibits DDR signaling in primary CD34$^+$ AML cells, primary murine Lin$^-$ BM cells, and human leukemic cell lines. (A) p(Ser1981)-ATM (*p*-ATM) and γ-H2AX were evaluated in CD34$^+$ AML blast cells isolated from the PB and BM of 6 AML patients by IF microscopy (×63). Treatment with 0.5 μM PKRI for 8 hours increased *p*-ATM and γ-H2AX staining, both 30 minutes after 5 Gy IR. Images are of CD34$^+$ cells from a single AML patient sample that are representative of results from 6 AML patients. (B-C) The percent of primary CD34$^+$ AML blasts cells positive for *p*-ATM (B) and p(Ser343)-NBS1 (*p*-NBS1) (C) after 5 Gy IR was increased by 8 hours of treatment with 0.5 μM PKRI as measured by flow cytometry. Results are an average of CD34$^+$ AML cells from 6 patients. (D) At the indicated times following 5 Gy IR treatment, primary CD34$^+$ AML cells treated with PKRI displayed an increased rate and extent of γ-H2AX foci formation following IR. The number of γ-H2AX foci per cell was counted by IF microscopy of 30 randomly selected cells for each AML patient sample and the averages graphed. (E-F) Quantitative real-time polymerase chain reaction was used to measure PKR expression in CD34$^+$ AML blasts from 6 patients relative to healthy donor CD34$^+$ BM cells. The percent of γ-H2AX (E) or *p*-ATM positive (F) cells 30 minutes after 5 Gy IR was measured by flow cytometry and plotted against the relative quantity (RQ) of PKR expression for each of the 6 AML patient samples. (G-H) Treatment of primary human CD34$^+$ cells isolated from BM of healthy donors with 0.5 μM PKRI for 8 hours increased the percentage of cells positive for γ-H2AX (G) and *p*-ATM (H) after 5 Gy IR as measured using flow cytometry. Results are an average of 3 independent experiments. (I) Lin$^-$ BM cells were isolated from WT, PKRKO, or TgPKR mice and irradiated with 5 Gy. At the indicated times after IR, the percent of cells positive for γ-H2AX was measured by flow cytometry. (J) *p*-ATM and (K) *p*-NBS1 were decreased in Lin$^-$ cells from BM of TgPKR mice compared with cells from WT mice. (L) Western blotting of REH cells demonstrates that *p*-ATM and *p*-NBS1 are increased in cells with reduced PKR expression by shRNA knockdown (sh-PKR) compared with cells expressing a control shRNA (sh-ctrl), both under normal growth conditions and 30 minutes after treatment with 5 Gy IR. (M) REH cells pretreated with PKRI (0.5 μM for 8 hours), IFN-γ (10 ng/mL for 24 hours), or poly(I:C) (5 μg/mL for 6 hours) demonstrate that increased PKR expression and activity decreased *p*-ATM and *p*-NBS1 30 minutes after IR. *$P < .05$; **$P < .01$. DAPI, 4,6 diamidino-2-phenylindole; M.W., molecular weight.

(Figure 2L and supplemental Figure 3L-R). Furthermore, inhibition of PKR activity by PKRI treatment also promoted increased *p*-ATM and *p*-NBS1 after IR (Figure 2M, lane 4 vs lane 2). In contrast, treatment of cells with either poly(I:C), a double-stranded RNA activator of PKR, or interferon (IFN)-γ, to increase PKR expression, significantly reduced the level of *p*-ATM and *p*-NBS1 following IR and delayed γ-H2AX formation (Figure 2M, lanes 6 and 8 vs lane 2, and supplemental Figure 3S-T). These results indicate that PKR kinase activity has a previously unrecognized role to antagonize DDR signaling in primary human and mouse hematopoietic cells as well as in leukemic cell lines.

Activated PKR associates with and inhibits ATM

Next, we tested whether PKR was a component of any ATM-containing complex by reciprocal co-IP. PKR co-IPs with ATM under normal growth conditions and PKRI treatment decreased, whereas poly(I:C) increased PKR-ATM co-precipitation (Figure 3A).

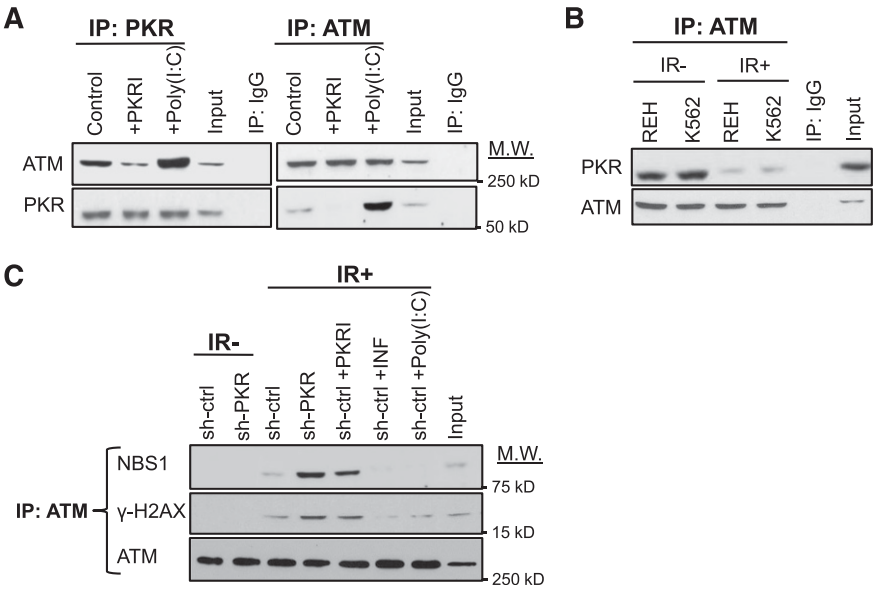

Figure 3. Activated PKR associates with ATM and inhibits ATM activation. (A) Western blotting after reciprocal co-IP of ATM and PKR from lysates of REH cells treated with either 0.5 μM PKRI for 8 hours or 5 μg/mL poly (I:C) for 6 hours demonstrates that PKR activity enhances PKR-ATM association. Input is 10% of total lysate used in the co-IP. Nonspecific IgG antibody was used as a negative co-IP control. (B) Western blotting indicates that co-IP of ATM and PKR is decreased at 30 minutes after 5 Gy IR. (C) co-IP of ATM with NBS1 or γ-H2AX is increased in REH cells by inhibition of PKR expression or activity, whereas cells treated with 10 ng/mL IFN-γ or 5 μg/mL poly(I:C) to increase PKR expression/activity have a decreased co-IP of ATM with either NBS1 or γ-H2AX.

Importantly, a significant reduction of PKR-ATM co-precipitation was observed after IR (Figure 3B). Furthermore, inhibition of PKR expression or activity promoted co-IP of ATM with NBS1 or γ-H2AX following IR (Figure 3C, lanes 4 and 5 vs lane 3). In contrast, treatment with poly(I:C) or IFN-γ greatly reduced association of these proteins (Figure 3C, lanes 6 and 7 vs lane 3), strongly suggesting that activated PKR interacts with ATM to antagonize ATM activation and association with downstream targets.

Nuclear PKR promotes PP2A-dependent ATM dephosphorylation

Our laboratory and others have demonstrated that PKR can activate PP2A, which has been reported to inhibit autophosphorylation and activation of ATM.[8,9,11,28] Thus, we tested whether nuclear PKR may inhibit ATM by a mechanism dependent on PP2A.

PKR efficiently co-precipitated with PP2A from the nuclear fraction of REH and K562 cell lysates, and this interaction was significantly decreased following IR (Figure 4A). Furthermore, cells with knocked-down PKR expression (sh-PKR) had an approximately twofold decrease in nuclear PP2A activity, suggesting that PKR is necessary to maintain steady-state nuclear PP2A activity (Figure 4B). Significantly, the association of ATM and PP2A is decreased in sh-PKR knockdown cells under normal growth conditions and to an even greater extent following IR (Figure 4C, lane 2 vs lane 1 and lane 5 vs lane 4). In all cases, decreased PP2A-ATM association was concomitant with increased *p*-ATM in nuclear extracts (Figure 4C). Furthermore, treatment of sh-PKR cells with the PP2A activator, FTY720, restored PP2A co-precipitation with ATM and reduced *p*-ATM to a level similar to that of control cells (Figure 4C, lane 3 vs lane 2 and lane 6 vs lane 5). Furthermore, although activation of PP2A activity by FTY720 promoted, inhibition of PP2A activity by OA decreased PKR-ATM association in nuclear extracts, suggesting that PKR-ATM association requires PP2A activity (Figure 4D). These results indicate that nuclear PKR promotes PP2A-ATM interaction, which antagonizes ATM autophosphorylation.

Because PP2A regulatory B subunits may be a downstream target of PKR, and IR has been reported to induce dissociation of the PP2A B55α subunit from the nuclear PP2A heterotrimer, we tested whether PKR may regulate nuclear B55α.[8,9,11,28,29] Following IR, B55α decreased in the nucleus and increased in the cytoplasm (Figure 4E, lane 1 vs 3 and lane 5 vs 7). Furthermore, sh-PKR cells had markedly decreased nuclear B55α that was even more evident following IR compared with control nuclear extracts (Figure 4E, lane 2 vs 1 and lane 4 vs 3). Significantly, when B55α expression was knocked down (Figure 4F, sh-B55α), cells with reduced B55α displayed increased γ-H2AX and *p*-ATM following IR compared with control (sh-ctrl) cells (Figure 4G, lane 5 vs 2 and Figure 4H). Furthermore, inhibition of PKR activity by PKRI treatment failed to promote γ-H2AX or *p*-ATM following IR in sh-B55α cells as it did in control cells (Figure 4G, lane 6 vs 3 and Figure 4H). Thus, nuclear PKR suppresses ATM autophosphorylation by promoting nuclear localization of B55α and activation of PP2A (Figure 4I).

Inhibition of PKR promotes more rapid kinetics of DNA double-strand break (DSB) repair

Next, we measured whether PKR may also delay the kinetics of DNA DSB repair using a neutral Comet assay to specifically detect DSBs.[30] At various times following IR, DNA damage was measured by calculating the average Olive Tail Moment of 50 randomly chosen cells.[31,32] Significantly, primary $CD34^+$ AML cells treated with PKRI displayed a more rapid and complete repair of DSBs 24 hours after irradiation than untreated control cells (Figure 5A-B). Similarly, 24 hours after IR, REH sh-PKR cells also displayed significantly more rapid resolution of Comet tails compared with control cells (Figure 5C-D). In addition, Lin^- BM cells from TgPKR mice had a significant delay in DSB repair, whereas Lin^- BM cells from PKRKO mice demonstrated faster kinetics of DSB repair after IR compared with WT cells (Figure 5E). Furthermore, treatment of TgPKR cells with PKRI promoted an increased efficiency of DSB repair similar to the level of PKRKO cells (Figure 5E). These data indicate that inhibition of PKR expression/activity can promote more rapid DSB repair following IR.

PKR accelerates leukemogenesis in a mouse model of leukemia

To determine whether increased PKR may accelerate leukemia progression, we crossed TgPKR or PKRKO mice with the NHD13 mouse model of leukemia to produce NHD13-TgPKR and NHD13-PKRKO mice.[3,33,34] The highly penetrant NHD13 model simulates high-risk human MDS that evolves to acute leukemia in ~60% of mice by 14 months.[33,34] Our laboratory and others have reported that leukemic transformation of NHD13 mice is accompanied by progressive genomic

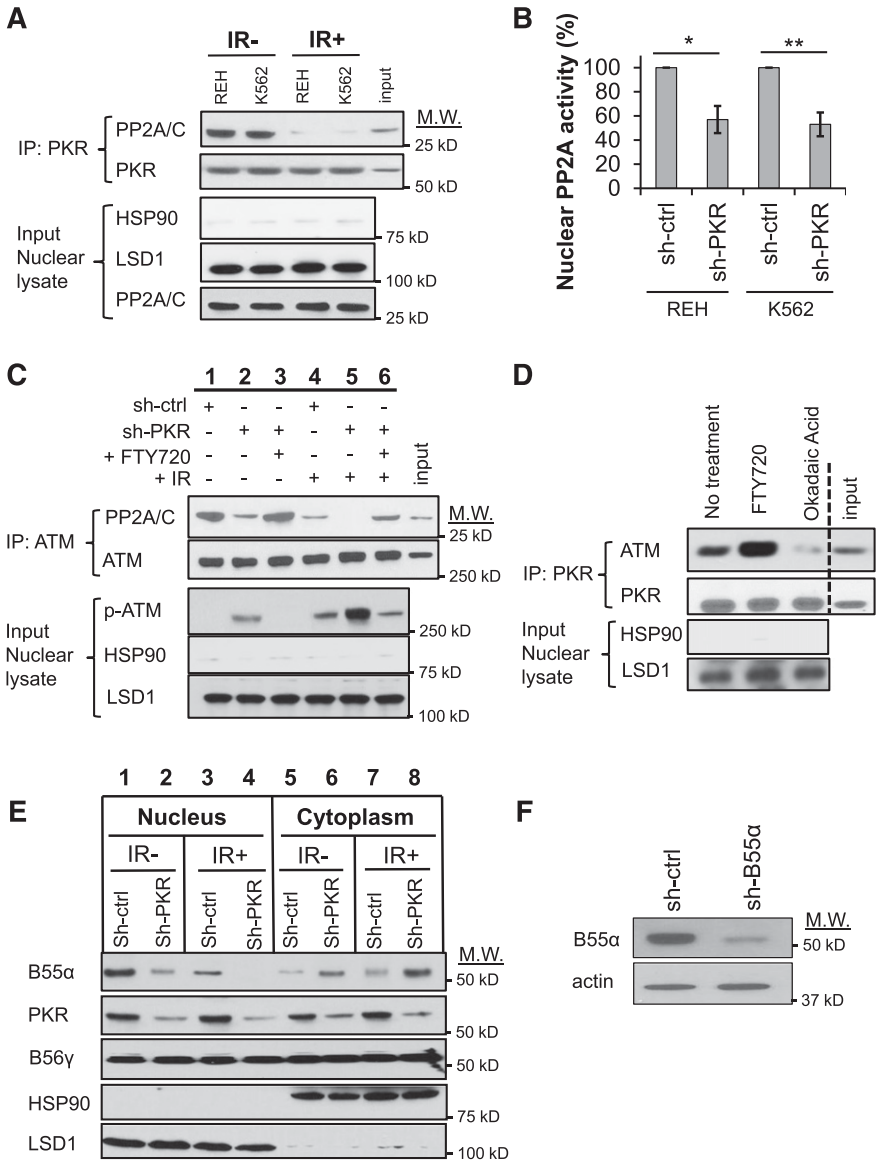

Figure 4. Nuclear PKR activates PP2A to inhibit ATM phosphorylation. (A) PKR co-IPs with PP2A from the nuclear fraction of REH and K562 cell lysates but this association is significantly reduced 30 minutes after exposure to 5 Gy IR (IR+). Western blotting for HSP90 (cytoplasm) and LSD1 (nucleus) was performed as a subcellular fractionation control. Input is 10% of total REH nuclear lysate used in the co-IP. (B) PP2A activity in the nuclear fraction of leukemia cell lines is reduced in cells with decreased PKR expression (sh-PKR) compared with cells transfected with a control shRNA (sh-ctrl). (C) co-IP of PP2A and ATM from the nuclear lysate of REH sh-ctrl and REH sh-PKR cells 30 minutes after treatment with 5 Gy IR and/or pretreatment with 2.5 μM of the PP2A activator FTY720 for 8 hours revealed that PP2A and ATM association is decreased after irradiation, decreased by reduced PKR expression, but increased by FTY720 treatment. In addition, *p*-ATM is correspondingly increased when ATM-PP2A nuclear association is decreased. Input is 10% of total REH sh-ctrl nuclear lysate used in the co-IP. (D) co-IP of PKR with ATM from the nuclear fraction of REH cells is increased by treatment with 2.5 μM of the PP2A activator FTY720 for 8 hours, whereas PKR-ATM association is decreased by treatment with 1 μM of the PP2A inhibitor OA for 8 hours. Vertical dashed line indicates a repositioned gel lane. (E) Expression of PP2A-B55α and PP2A-B56γ subunits in the cytoplasm and nucleus of REH cells were detected by western blotting. Knockdown of PKR decreased nuclear B55α and increased cytoplasmic B55α both before and after 5 Gy IR. (F) Western blotting demonstrates that B55α expression in REH cells was decreased by B55α-specific shRNA (sh-B55α) compared with control shRNA (sh-ctrl) cells. (G) γ-H2AX formation 30 minutes after 5 Gy IR was measured by western blotting. Pretreatment of cells with 0.5 μM PKRI for 8 hours prior to IR promotes γ-H2AX formation in REH sh-ctrl cells but not REH sh-B55α cells with decreased B55α expression. (H) Flow cytometry after IR reveals that PKRI promotes increased *p*-ATM in control REH cells (sh-ctrl) but not B55α knockdown cells (sh-B55α). (I) Proposed model by which nuclear PKR mediates PP2A activity and DDR signaling following IR. In undamaged cells, nuclear PKR indirectly antagonizes ATM activation by promoting nuclear localization of the PP2A B55α regulatory subunit that increases nuclear PP2A phosphatase activity to inhibit ATM autophosphorylation. Following IR, PKR and PP2A no longer interact with the ATM complex, and the PP2A-B55α subunit is sequestered in the cytoplasm allowing ATM to be activated and initiate DDR signaling events. $^{*}P < .05$; $^{**}P < .01$.

instability and the accumulation of collaborating oncogenic mutations.[35,36] NHD13, NHD13-TgPKR, and NHD13-PKRKO mice were aged until death or physical deterioration requiring euthanasia. Acute leukemia was identified by high PB white blood count ($\geq 20 \times 10^3/\mu L$), ≥20% BM blasts, increased BM cellularity with loss of differentiation, and a clonal population of immature cells detected by flow cytometry (supplemental Figure 4A).

The OS of NHD13-TgPKR mice were significantly shorter, whereas the survival of NHD13-PKRKO mice were significantly longer than that of NHD13 mice (Figure 6A). Furthermore, NHD13-TgPKR mice had a higher incidence of leukemia than the NHD13 mice (Figure 6B). Conversely, KO of PKR delayed but did not prevent leukemia development (Figure 6A-B). In addition, endogenous PKR expression was significantly increased (RQ >2) with age in NHD13 mice

Figure 4. (Continued).

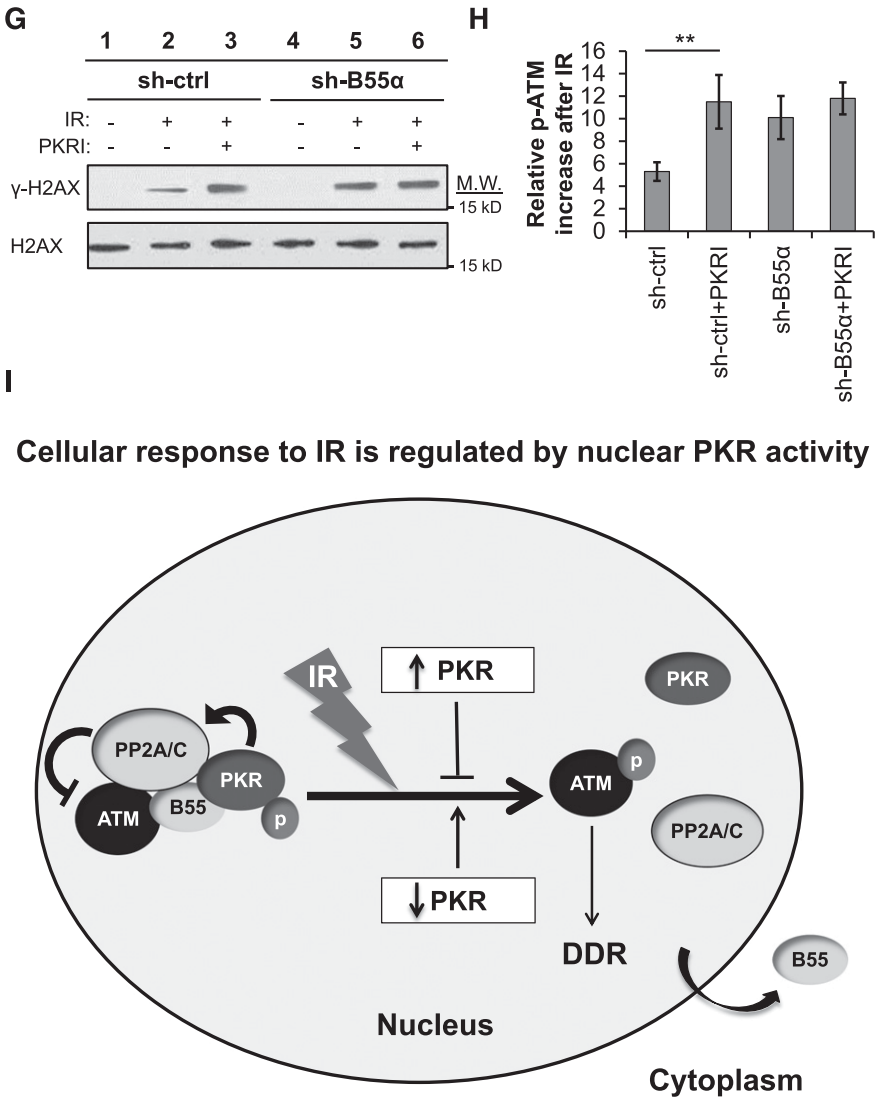

that developed acute leukemia and had shortened survival (Figure 6C and supplemental Figure 4B). When BM of mice was examined at a time prior to the development of acute leukemia, NHD13 mice exhibited an age-associated increase in BM blasts that was further elevated by the PKR transgene (Figure 6D). In contrast, at 6 months of age, the NHD13-PKRKO mice had significantly reduced BM blasts and increased colony-forming unit (CFU)-granulocyte, erythrocyte, monocyte, megakaryocyte (GEMM) frequency compared with NHD13 mice (Figure 6E). Consequently, PKRKO mice demonstrated increased PB cell counts and reduced inhibition of myeloid differentiation (supplemental Figure 4C-K). Furthermore, endogenous PKR expression in Lin^- BM cells of NHD13 mice was inversely proportional to *p*-ATM and γ-H2AX after IR (Figure 6F and supplemental Figure 4L). Collectively, these results indicate that increased PKR expression may cooperate with the NHD13 oncogene to accelerate the accumulation of mutations that lead to more rapid MDS evolution to acute leukemia.

PKR inhibition prevents the accumulation of somatic mutations in vivo

Because PKR inhibition promoted DDR signaling and DSB repair in vitro, we tested whether PKR may affect the frequency of somatic mutations in vivo. Mutation frequency was measured using the *PIG-A* assay that detects loss of CD24 on murine reticulocytes and is representative of spontaneous mutations that occur in hematopoietic stem and progenitor cells.[35,37,38]

At all ages examined, reticulocytes from TgPKR mice had a significantly increased *PIG-A* mutation frequency compared with WT mice (Figure 7A). Furthermore, the age-associated increase in mutation frequency from 3 to 12 months was enhanced by TgPKR but significantly reduced by KO of PKR (Figure 7A). Similarly, PB cells of NHD13-TgPKR mice demonstrated a significantly higher age-associated increase of the *PIG-A* mutation frequency, whereas those of NHD13-PKRKO mice were significantly reduced compared with NHD13 mice (Figure 7B). In addition, reticulocytes of TgPKR mice had a significantly greater mutation frequency than WT mice at Week 1 after IR and did not recover to the low mutation frequency observed in WT mice at Week 4 after IR (Figure 7C). In contrast, PKRKO mice displayed a reduced mutation frequency compared with WT mice following IR (Figure 7C). Thus, increased PKR expression promoted a mutator phenotype, whereas KO of PKR expression reduced the frequency of mutations in vivo.

Next, we tested whether in vivo pharmacologic inhibition of PKR can reduce the mutation frequency in hematopoietic cells of mice. The administration of PKRI to mice inhibited PKR activity, but not total PKR expression or activity of the related kinase PERK, in Lin^- BM

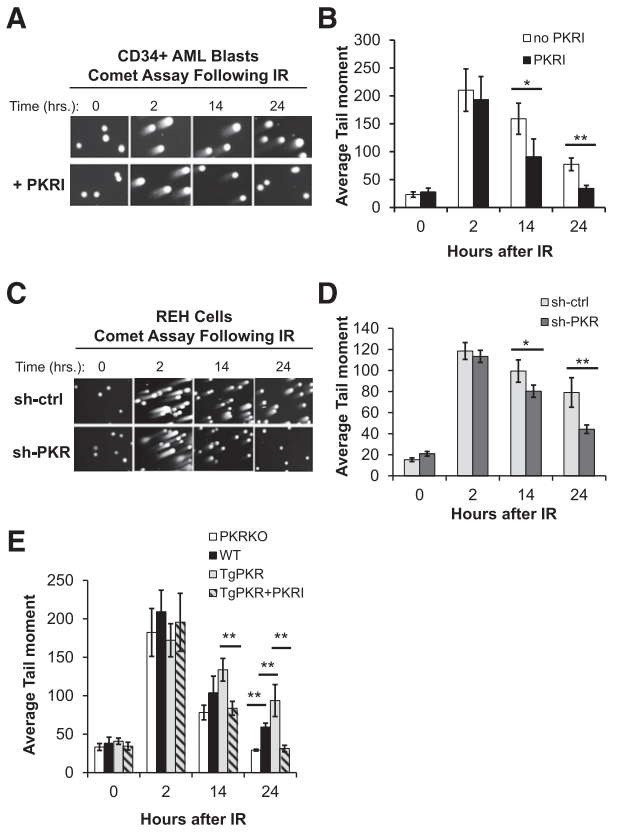

Figure 5. Inhibition of PKR expression or activity promotes DNA DSB repair in hematopoietic cells. Neutral Comet assays were used to measure DNA DSB repair following 5 Gy IR. (A) Inhibition of PKR by treatment with 0.5 μM PKRI prior to and following IR promoted faster kinetics of DNA DSB repair in primary $CD34^+$ AML cells. SYBR gold-stained Comets were visualized by microscopy (×40). A representative Comet assay of 1 patient sample is shown. (B) The average Comet Olive Tail Moment from 50 randomly chosen $CD34^+$ AML cells in each of 6 patient samples was determined. (C) Representative Comet assay, and (D) calculation of the average Comet Tail Moment of 50 randomly chosen REH cells demonstrates reduced PKR expression (sh-PKR) increases the rate of DNA DSB repair compared with control (sh-ctrl) cells. (E) Lin^- BM cells were collected from WT, TgPKR, and PKRKO mice, and treated with 5 Gy IR. Comet Tail Moments were calculated from 50 randomly chosen cells for each genotype. Lin^- BM cells from PKRKO mice displayed more rapid kinetics of DNA DSB repair than WT cells. Compared with WT, TgPKR cells exhibit delayed DNA DSB repair that can be restored by treatment with 0.5 μM PKRI. $^*P < .05$; $^{**}P < .01$.

cells (supplemental Figure 5A-C). Significantly, PKRI treatment reduced the *PIG-A* mutation frequency in PB reticulocytes from IR-treated mice (Figure 7D). Furthermore, when PKRI was administered continuously to NHD13 mice for 28 days, the mutation frequency in PB reticulocytes were reduced compared with vehicle-treated mice, and BM from PKRI-treated NHD13 mice had significantly improved CFU-GEMM activity (Figure 7E-F). In addition, PKRI treatment of NHD13 mice promoted a significant improvement in PB cell counts and animal weight (supplemental Figure 5D-F and data not shown). Thus, pharmacologic inhibition of PKR activity seemingly prevents the accumulation of potentially deleterious mutations in the NHD13 model.

Discussion

Our results demonstrate that nuclear PKR has an unexpected pro-oncogenic function to inhibit DDR signaling and DSB repair that can lead to the accumulation of age-associated or irradiation-induced somatic mutations. PKR expression was inversely proportional to both ATM autophosphorylation/activation and phosphorylation of ATM downstream targets following IR in primary $CD34^+$ cells, Lin^- BM cells from mouse models, and established leukemia cell lines. Furthermore, inhibition of PKR expression or activity in all of these cells promoted a more rapid DDR signaling and DSB repair following IR. Consistent with these observations, TgPKR but not PKRKO mice demonstrated a mutator phenotype characterized by increased radiation-induced or age-associated mutation frequency in hematopoietic cells. Furthermore, the accumulation of somatic mutations that occurs in the NHD13 mouse model of MDS/acute leukemia upon aging was significantly elevated by co-expression of the PKR transgene, whereas

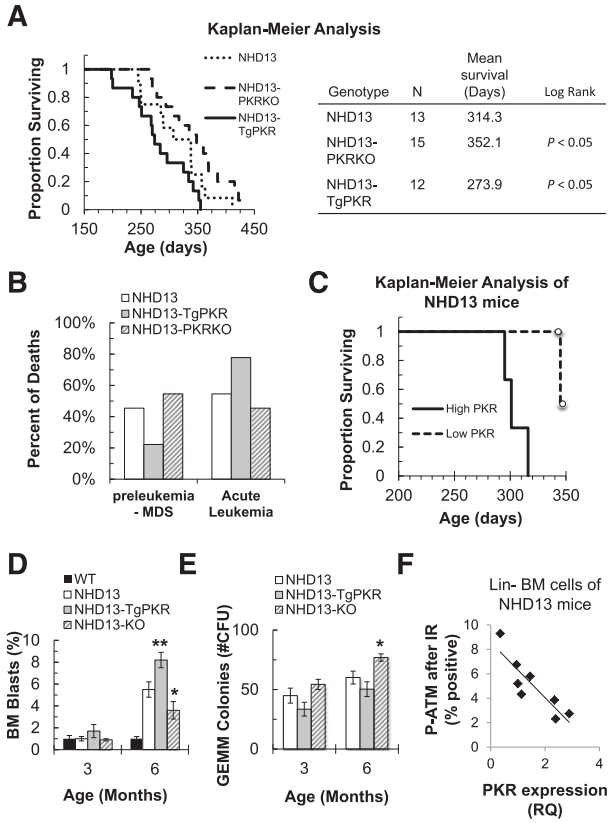

Figure 6. PKR expression cooperates with the NHD13 transgene to shorten survival and promote MDS evolution to acute leukemia in the NHD13 mouse. (A) NHD13 mice were crossed with mice expressing a PKR transgene specifically in hematopoietic cells (TgPKR) or PKRKO mice, to produce NHD13-TgPKR and NHD13-PKRKO mice. NHD13 (n = 12), NHD13-TgPKR (n = 12), and NHD13-PKRKO (n = 12) mice were aged until physical deterioration led to death or required euthanasia (defined as body condition score ≤2). (A) Kaplan–Meier analysis demonstrates that PKR expression cooperates with NHD13 to significantly shorten the survival of mice. (B) NHD13-TgPKR mice more frequently die of acute leukemia than NHD13 mice. Acute leukemia or MDS was determined by hematoxylin and eosin staining and flow cytometry of BM cells collected at time of death. (C) Kaplan–Meier analysis demonstrates superior survival in NHD13 mice with low-level PKR expression vs NHD13 mice with high-level PKR expression (RQ >2) relative to age-matched WT controls. PKR expression in PB mononuclear cells collected as NHD13 mice aged was measured by quantitative real-time polymerase chain reaction. Circles represent mice that were censored at 350 days. (D-E) At 3 and 6 months of age, BM was collected from WT, NHD13, NHD13-TgPKR, and NHD13-PKRKO mice for comparison by flow cytometry analysis. (D) BM blasts were measured using $CD45^+$ expression and side scatter. NHD13-TgPKR mice had significantly increased BM blasts compared with NHD13 mice at 6 months, whereas in PKRKO mice, this was significantly reduced. (E) BM from NHD13-PKRKO mice had significantly increased CFU-GEMM activity compared with NHD13 or NHD13-TgPKR. (F) Lin^- BM cells were isolated from 8 NHD13 mice and PKR level determined by flow cytometry. Some 30 minutes after IR, *p*-ATM was measured by flow cytometry and plotted vs PKR expression to reveal that relative PKR expression was inversely proportional to *p*-ATM. Each point represents an individual mouse. $^*P < .05$; $^{**}P < .01$.

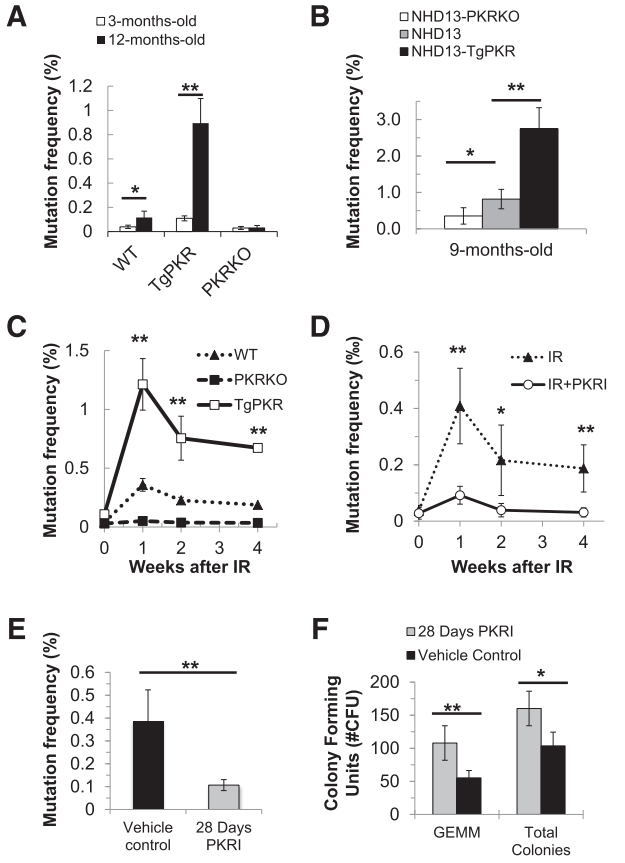

Figure 7. Inhibition of PKR protects against mutations induced by age, IR, or a potent oncogene. The mutation frequency was measured serially in PB reticulocytes using the in vivo PIG-A mutation assay that detects the loss of the glycosylphosphatidylinositol-linked proteins like CD24 on the surface of reticulocytes by flow cytometry. The PIG-A mutation frequency was calculated as the percentage of $CD24^-$ reticulocytes/total reticulocytes analyzed. (A) PB from unperturbed young (3-month-old) vs old (12-month-old) WT, PKRKO, and TgPKR mice was obtained, and reticulocytes isolated and analyzed by flow cytometry for the presence or absence of CD24. Increased PKR expression in TgPKR hematopoietic cells promotes an age-associated increase in the frequency of PIG-A mutation compared with WT or PKRKO. (B) NHD13-TgPKR mice, aged 9 months, have a significantly increased frequency of PIG-A mutation compared with NHD13 or NHD13-PKRKO mice. (C) Increased PKR expression promotes a significant increase in the frequency of PIG-A mutations following 5 Gy IR exposure. (D) PKRI treatment reduces the frequency of PIG-A somatic mutation in PB cells of mice following IR. WT mice were injected intraperitoneally with either 200 μg/kg PKRI or PBS (5 mice in each treatment group) and administered a single sublethal dose of IR (5 Gy). After IR, mice received either 200 μg/kg PKRI or PBS every 12 hours for 4 weeks. (E-F) NHD13 mice that were 4 months old were implanted with Alzet osmotic pumps (#1004) filled with either PKRI (1.5 mg/mL in PBS:dimethylsulfoxide) or vehicle control (PBS:dimethylsulfoxide). After 28 days, mice were euthanized to collect blood and BM. (E) The PIG-A mutation frequency in PB of NHD13 mice was significantly reduced by 28-day continuous PKRI treatment. (F) BM of NHD13 mice that received continuous PKRI treatment had significantly greater CFU-GEMM and total CFU activity. $^*P < .05$; $^{**}P < .01$.

KO of PKR expression or pharmacologic inhibition of PKR activity reduced the frequency of spontaneous mutations in vivo. Thus, PKR cooperated with the NHD13 transgene to accelerate leukemia progression leading to shortened survival. Significantly, high PKR expression was associated with poor OS and shortened remission duration for AML patients, and correlated with worse survival in breast, lung, and ovarian cancer patients (supplemental Figure 5).[13-15,39-41] Although it is unclear how PKR may be upregulated in cancer patients and mice, chronic inflammatory stress may contribute since PKR has been well characterized as an IFN-inducible gene. Significantly, findings here suggest that patients with relatively high PKR expression may have inferior clinical outcomes due to the cooperating oncogenic role of PKR to promote the accumulation of potentially deleterious mutations and accelerate leukemogenesis. These findings suggest that PKR inhibition may represent a novel therapeutic strategy to prevent/delay leukemia progression and potentially tumorigenesis of other cancers.

Our findings demonstrate that PKR has an important and previously unrecognized nuclear function to antagonize ATM activation. Significantly, ATM and PKR co-precipitated in nuclear extracts, and PKR activity was required for this interaction. Furthermore, the PKR-ATM association was lost upon irradiation. Our findings suggest that PKR antagonizes ATM function by activating PP2A. Other reports suggest that PP2A maintains ATM in a catalytically quiescent state in undamaged cells.[28,42] Significantly, we observed that PKR inhibition reduced nuclear PP2A activity and nuclear localization of the PP2A B55α regulatory subunit. Whether B55α is a direct downstream target of PKR remains undetermined. In addition, knockdown of PKR resulted in reduced co-precipitation of ATM with PP2A, implying that PKR may regulate PP2A-ATM interaction. Thus, we propose that PKR promotes nuclear B55α localization necessary for nuclear PP2A activity and PP2A-ATM association, which functionally suppresses ATM autophosphorylation in undamaged cells. In response to genotoxic stress including IR, PP2A and ATM rapidly dissociate, allowing ATM autophosphorylation and initiation of the DDR signaling cascade (Figure 4I). These results have now prompted us to reinterpret previous findings that inhibition of PKR promotes cell survival following treatment with genotoxic agents, such as doxorubicin, exclusively due to decreased apoptosis. We now propose that inhibition of PKR expression/activity may also promote increased cell survival due to an improved DNA repair capacity that results in a more effective response to genotoxic stress. Significantly, these results suggest that increased PKR expression/activity, such as observed in acute leukemia and other cancers, may cooperate with other more potent oncogenes to accelerate tumorigenesis.

Acknowledgments

The authors thank Dr Ying Li for flow cytometry assistance and Dr Christopher Carter for immunohistochemistry interpretation.

This study was supported by the National Institutes of Health (NIH) National Heart, Lung, and Blood Institute (R01 HL054083), the Florida Department of Health Bankhead-Coley award (09BW-06), a University of Florida Health Cancer Center Team Science award, and University of Florida Gatorade funding. X.C. was supported in part by the NIH National Institute of Diabetes and Digestive and Kidney Diseases (T32 DK074367). M.B. was supported in part by the NIH National Center for Research Resources Clinical and Translational Science Awards grant (UL1 TR000064).

Authorship

Contribution: M.B. and X.C. performed research, analyzed data, and wrote the manuscript; K.D.B. designed experiments and analyzed results; M.Y.K. provided key reagents; S.M.K. performed experiments and analyzed results; and R.L.B. and W.S.M. designed experiments, analyzed data, and wrote the manuscript.

Conflict-of-interest disclosure: The authors declare no competing financial interests.

Correspondence: W. Stratford May, Division of Hematology and Oncology, Department of Medicine, University of Florida, 2033 Mowry Rd, Box 103633, Gainesville, FL 32610; e-mail: smay@ufl.edu.

References

1. Bennett RL, Blalock WL, Abtahi DM, Pan Y, Moyer SA, May WS. RAX, the PKR activator, sensitizes cells to inflammatory cytokines, serum withdrawal, chemotherapy, and viral infection. *Blood.* 2006;108(3):821-829.
2. Ito T, Jagus R, May WS. Interleukin 3 stimulates protein synthesis by regulating double-stranded RNA-dependent protein kinase. *Proc Natl Acad Sci USA.* 1994;91(16):7455-7459.
3. Liu X, Bennett RL, Cheng X, Byrne M, Reinhard MK, May WS Jr. PKR regulates proliferation, differentiation, and survival of murine hematopoietic stem/progenitor cells. *Blood.* 2013; 121(17):3364-3374.
4. Bennett RL, Pan Y, Christian J, Hui T, May WS Jr. The RAX/PACT-PKR stress response pathway promotes p53 sumoylation and activation, leading to G_1 arrest. *Cell Cycle.* 2012;11(2):407-417.
5. Cuddihy AR, Li S, Tam NW, et al. Double-stranded-RNA-activated protein kinase PKR enhances transcriptional activation by tumor suppressor p53. *Mol Cell Biol.* 1999;19(4): 2475-2484.
6. Cuddihy AR, Wong AH, Tam NW, Li S, Koromilas AE. The double-stranded RNA activated protein kinase PKR physically associates with the tumor suppressor p53 protein and phosphorylates human p53 on serine 392 in vitro. *Oncogene.* 1999;18(17):2690-2702.
7. Dar AC, Dever TE, Sicheri F. Higher-order substrate recognition of eIF2alpha by the RNA-dependent protein kinase PKR. *Cell.* 2005; 122(6):887-900.
8. Ruvolo VR, Kurinna SM, Karanjeet KB, et al. PKR regulates B56(alpha)-mediated BCL2 phosphatase activity in acute lymphoblastic leukemia-derived REH cells. *J Biol Chem.* 2008; 283(51):35474-35485.
9. Xu Z, Williams BR. The B56alpha regulatory subunit of protein phosphatase 2A is a target for regulation by double-stranded RNA-dependent protein kinase PKR. *Mol Cell Biol.* 2000;20(14): 5285-5299.
10. Donzé O, Deng J, Curran J, Sladek R, Picard D, Sonenberg N. The protein kinase PKR: a molecular clock that sequentially activates survival and death programs. *EMBO J.* 2004; 23(3):564-571.
11. Cheng X, Bennett RL, Liu X, Byrne M, May WS Jr. PKR negatively regulates leukemia progression in association with PP2A activation, Bcl-2 inhbition and increased apoptosis. *Blood Cancer J.* 2013;3: e144.
12. Yang YL, Reis LF, Pavlovic J, et al. Deficient signaling in mice devoid of double-stranded RNA-dependent protein kinase. *EMBO J.* 1995;14(24): 6095-6106.
13. Bennett RL, Carruthers AL, Hui T, Kerney KR, Liu X, May WS Jr. Increased expression of the dsRNA-activated protein kinase PKR in breast cancer promotes sensitivity to doxorubicin. *PLoS One.* 2012;7(9):e46040.
14. Kim SH, Gunnery S, Choe JK, Mathews MB. Neoplastic progression in melanoma and colon cancer is associated with increased expression and activity of the interferon-inducible protein kinase, PKR. *Oncogene.* 2002;21(57):8741-8748.
15. Kim SH, Forman AP, Mathews MB, Gunnery S. Human breast cancer cells contain elevated levels and activity of the protein kinase, PKR. *Oncogene.* 2000;19(27):3086-3094.
16. Basu S, Panayiotidis P, Hart SM, et al. Role of double-stranded RNA-activated protein kinase in human hematological malignancies. *Cancer Res.* 1997;57(5):943-947.
17. Blalock WL, Grimaldi C, Fala F, et al. PKR activity is required for acute leukemic cell maintenance and growth: a role for PKR-mediated phosphatase activity to regulate GSK-3 phosphorylation. *J Cell Physiol.* 2009;221(1):232-241.
18. Jeffrey IW, Kadereit S, Meurs EF, et al. Nuclear localization of the interferon-inducible protein kinase PKR in human cells and transfected mouse cells. *Exp Cell Res.* 1995;218(1):17-27.
19. Follo MY, Finelli C, Mongiorgi S, et al. PKR is activated in MDS patients and its subcellular localization depends on disease severity. *Leukemia.* 2008;22(12):2267-2269.
20. Blalock WL, Bavelloni A, Piazzi M, et al. Multiple forms of PKR present in the nuclei of acute leukemia cells represent an active kinase that is responsive to stress. *Leukemia.* 2011;25(2): 236-245.
21. Kornblau SM, Qiu YH, Zhang N, et al. Abnormal expression of FLI1 protein is an adverse prognostic factor in acute myeloid leukemia. *Blood.* 2011;118(20):5604-5612.
22. Kornblau SM, Coombes KR. Use of reverse phase protein microarrays to study protein expression in leukemia: technical and methodological lessons learned. *Methods Mol Biol.* 2011;785:141-155.
23. Tibes R, Qiu Y, Lu Y, et al. Reverse phase protein array: validation of a novel proteomic technology and utility for analysis of primary leukemia specimens and hematopoietic stem cells. *Mol Cancer Ther.* 2006;5(10):2512-2521.
24. Dickey JS, Redon CE, Nakamura AJ, Baird BJ, Sedelnikova OA, Bonner WM. H2AX: functional roles and potential applications. *Chromosoma.* 2009;118(6):683-692.
25. Pilch DR, Sedelnikova OA, Redon C, Celeste A, Nussenzweig A, Bonner WM. Characteristics of gamma-H2AX foci at DNA double-strand breaks sites. *Biochem Cell Biol.* 2003;81(3):123-129.
26. Lim DS, Kim ST, Xu B, et al. ATM phosphorylates p95/nbs1 in an S-phase checkpoint pathway. *Nature.* 2000;404(6778):613-617.
27. Romano PR, Garcia-Barrio MT, Zhang X, et al. Autophosphorylation in the activation loop is required for full kinase activity in vivo of human and yeast eukaryotic initiation factor 2alpha kinases PKR and GCN2. *Mol Cell Biol.* 1998; 18(4):2282-2297.
28. Goodarzi AA, Jonnalagadda JC, Douglas P, et al. Autophosphorylation of ataxia-telangiectasia mutated is regulated by protein phosphatase 2A. *EMBO J.* 2004;23(22):4451-4461.
29. Guo CY, Brautigan DL, Larner JM. ATM-dependent dissociation of B55 regulatory subunit from nuclear PP2A in response to ionizing radiation. *J Biol Chem.* 2002;277(7):4839-4844.
30. Fairbairn DW, Olive PL, O'Neill KL. The comet assay: a comprehensive review. *Mutat Res.* 1995; 339(1):37-59.
31. Olive PL, Banáth JP. Radiation-induced DNA double-strand breaks produced in histone-depleted tumor cell nuclei measured using the neutral comet assay. *Radiat Res.* 1995;142(2): 144-152.
32. Lee E, Oh E, Lee J, Sul D, Lee J. Use of the tail moment of the lymphocytes to evaluate DNA damage in human biomonitoring studies. *Toxicol Sci.* 2004;81(1):121-132.
33. Slape C, Liu LY, Beachy S, Aplan PD. Leukemic transformation in mice expressing a NUP98-HOXD13 transgene is accompanied by spontaneous mutations in Nras, Kras, and Cbl. *Blood.* 2008;112(5):2017-2019.
34. Lin YW, Slape C, Zhang Z, Aplan PD. NUP98-HOXD13 transgenic mice develop a highly penetrant, severe myelodysplastic syndrome that progresses to acute leukemia. *Blood.* 2005; 106(1):287-295.
35. Byrne M, Bennett RL, Cheng X, May WS. Progressive genomic instability in the Nup98-HoxD13 model of MDS correlates with loss of the PIG-A gene product. *Neoplasia.* 2014;16(8): 627-633.
36. Chung YJ, Robert C, Gough SM, Rassool FV, Aplan PD. Oxidative stress leads to increased mutation frequency in a murine model of myelodysplastic syndrome. *Leuk Res.* 2014; 38(1):95-102.
37. Ohtani S, Unno A, Ushiyama A, Kimoto T, Miura D, Kunugita N. The in vivo Pig-a gene mutation assay is useful for evaluating the genotoxicity of ionizing radiation in mice. *Environ Mol Mutagen.* 2012;53(8): 579-588.
38. Peruzzi B, Araten DJ, Notaro R, Luzzatto L. The use of PIG-A as a sentinel gene for the study of the somatic mutation rate and of mutagenic agents in vivo. *Mutat Res.* 2010;705(1):3-10.
39. Terada T, Maeta H, Endo K, Ohta T. Protein expression of double-stranded RNA-activated protein kinase in thyroid carcinomas: correlations with histologic types, pathologic parameters, and Ki-67 labeling. *Hum Pathol.* 2000;31(7):817-821.
40. Hiasa Y, Kamegaya Y, Nuriya H, et al. Protein kinase R is increased and is functional in hepatitis C virus-related hepatocellular carcinoma. *Am J Gastroenterol.* 2003;98(11):2528-2534.
41. Roh MS, Kwak JY, Kim SJ, et al. Expression of double-stranded RNA-activated protein kinase in small-size peripheral adenocarcinoma of the lung. *Pathol Int.* 2005;55(11):688-693.
42. Bakkenist CJ, Kastan MB. DNA damage activates ATM through intermolecular autophosphorylation and dimer dissociation. *Nature.* 2003;421(6922): 499-506.